Immortalization of Human Alveolar Epithelial Cells to Investigate Nanoparticle Uptake

Sarah J. Kemp[1], Andrew J. Thorley[1], Julia Gorelik[1], Michael J. Seckl[2], Michael J. O'Hare[3], Alexandre Arcaro[4], Yuri Korchev[2], Peter Goldstraw[5], and Teresa D. Tetley[1]

[1]National Heart and Lung Institute, and [2]Division of Medicine, Imperial College, London, United Kingdom; [3]Department of Surgery, University College London, London, United Kingdom; [4]Division of Clinical Chemistry and Biochemistry, University Children's Hospital Zurich, Zurich, Switzerland; and [5]Department of Thoracic Surgery, Royal Brompton and Harefield NHS Trust, London, United Kingdom

Primary human alveolar type 2 (AT2) cells were immortalized by transduction with the catalytic subunit of telomerase and simian virus 40 large-tumor antigen. Characterization by immunochemical and morphologic methods demonstrated an AT1-like cell phenotype. Unlike primary AT2 cells, immortalized cells no longer expressed alkaline phosphatase, pro–surfactant protein C, and thyroid transcription factor-1, but expressed increased caveolin-1 and receptor for advanced glycation end products (RAGE). Live cell imaging using scanning ion conductance microscopy showed that the cuboidal primary AT2 cells were approximately 15 μm and enriched with surface microvilli, while the immortal AT1 cells were attenuated more than 40 μm, resembling these cells *in situ*. Transmission electron microscopy highlighted the attenuated morphology and showed endosomal vesicles in some immortal AT1 cells (but not primary AT2 cells) as found *in situ*. Particulate air pollution exacerbates cardiopulmonary disease. Interaction of ultrafine, nano-sized particles with the alveolar epithelium and/or translocation into the cardiovasculature may be a contributory factor. We hypothesized differential uptake of nanoparticles by AT1 and AT2 cells, depending on particle size and surface charge. Uptake of 50-nm and 1-μm fluorescent latex particles was investigated using confocal microscopy and scanning surface confocal microscopy of live cells. Fewer than 10% of primary AT2 cells internalized particles. In contrast, 75% immortal AT1 cells internalized negatively charged particles, while less than 55% of these cells internalized positively charged particles; charge, rather than size, mattered. The process was rapid: one-third of the total cell-associated negatively charged 50-nm particle fluorescence measured at 24 hours was internalized during the first hour. AT1 cells could be important in translocation of particles from the lung into the circulation.

Keywords: alveolar; epithelial; immortalization; nanoparticle; translocation

CLINICAL RELEVANCE

Immortal, human epithelial alveolar type (AT) 1 cells (not primary human AT2 cells) avidly internalized nanoparticles. These cells account for 95% of the alveolar surface area, and such interactions may contribute to the effects of ultrafine air pollution particles.

The alveolar epithelium consists of alveolar epithelial type I (AT1) and type II (AT2) cells. AT2 cells are secretory cells, synthesizing and releasing pulmonary surfactant, to maintain reduced surface tension, as well as producing antiproteases, antioxidants, surfactant proteins, defensins, cytokines/chemokines, and other molecules that are important in lung defense and maintaining pulmonary homeostasis. AT2 cells also maintain alveolar integrity by proliferation and differentiation into AT1 cells, which are, debatably, terminally differentiated (1). Although the cuboidal AT2 cells contribute approximately 60% of the total alveolar epithelial cells, the squamous AT1 cells cover over 95% of the alveolar surface, spreading to only 0.2 μm thick, providing a large surface area for gas exchange (2). Other functions of AT1 cells are less well known, although recent studies illustrate a role in protein transport and translocation via transcytosis (3). Understanding AT1 cell function has been hampered by the difficulty of isolating these cells to investigate *in vitro*. Many studies depend upon AT2 cell differentiation into AT1 cells *in vitro* over several days. However, these terminally differentiated cells cannot be passaged, and primary AT2 cells need to be isolated regularly.

Recently, AT1 cells have been isolated from rodent lung and have been shown to express the epithelial sodium channel, ENaC, and Na^+ and K^+ ATPase activity and are therefore well equipped to regulate fluid homeostasis (4, 5). Rat AT1 cells were shown to take up 2.5 times more Na^+ per μg of protein, compared with AT2 cells isolated from the same animals (5). This and other studies suggest that AT1 cells are as important as AT2 cells in lung fluid homoeostasis. Clearly it is necessary to further characterize AT1 cells to understand their role in pulmonary alveolar health and disease.

We have established methods to routinely isolate primary human AT2 cells from human lung tissue after lung resection (6). Previously, one author (M.J.O.) immortalized primary normal adult human mammary fibroblasts after transduction with the catalytic subunit of telomerase (hTERT) and a temperature-sensitive mutant of simian virus 40 large-tumor antigen (U19tsA58 LT) (7). One aim of the current study was to immortalize human AT2 cells to provide a regular source of human alveolar epithelial cells. Subsequent characterization of these immortalized human AT2 cells revealed that they expressed an AT1 cell–like phenotype.

The respiratory region is a significant target of inhaled particles with aerodynamic diameters below 10 μm (8). Peaks in particulate air pollution are associated with increased morbidity and mortality from cardiorespiratory disease (9, 10); *in vivo* studies suggest that there may be translocation of nano-sized particles into the circulation possibly due to epithelial uptake (11, 12). Thus, our second aim was to determine whether human alveolar epithelial cells internalize cell surface–modified fine and nano-sized particles.

(*Received in original form September 13, 2007 and in final form May 8, 2008*)

This research was supported by the Department of Health, London, the Biotechnology and Biological Sciences Research Council, the Department of the Environment, Fisheries and Rural Affairs, and the Medical Research Council, UK.

Correspondence and requests for reprints should be addressed to Teresa D. Tetley, BSc, PhD, Lung Cell Biology, National Heart and Lung Institute, Imperial College, London SW3 6LY, UK. E-mail: t.tetley@imperial.ac.uk

Am J Respir Cell Mol Biol Vol 39. pp 591–597, 2008
Originally Published in Press as DOI: 10.1165/rcmb.2007-0334OC on June 6, 2008
Internet address: www.atsjournals.org

MATERIALS AND METHODS

Isolation and Culture of Primary AT2 Cells

Primary human AT2 cells were isolated from normal regions of lung tissue after lobectomy for carcinoma, as described previously (6). Ethical approval was obtained from the Brompton, Harefield, and NHLI Ethics Committee, and patients gave informed consent. The primary AT2 cells were cultured on collagen type-1–coated plates in DCCM-1 (Biological Industries, Kibutz, Israel) containing 10% newborn calf serum (NCS), 100 U/ml penicillin, 100 μg/ml streptomycin, and 2 mM glutamine.

Immortalization of Primary AT2 Cells

Purified primary AT2 cells were immortalized as described by us previously (7). Thus, midconfluent, proliferating primary AT2 cell cultures were retrovirally transduced with hTERT and U19tsA58 LT. Cells that were successfully transduced were cultured in the same medium as the primary AT2 cells, supplemented with 0.5 mg/ml G418 (Sigma, Poole, UK).

Transmission Electron Microscopy

Immortal and primary cells were grown on clear polyester Transwell membranes (0.4 μm pores; Corning Life Sciences, Schipol RDK, The Netherlands). Confluent cells were fixed with 2.5% glutaraldehyde in cacodylate buffer and post-fixed in 1% osmium tetroxide, followed by dehydration through a graded series of ethanol concentrations. The membranes were embedded in Araldite before 1-μm and 100-nm sections were cut (ultracut E microtome; Reichert-Jung, Depew, New York). The 1-μm sections were stained with 1% toluidine blue and viewed using a light microscope (Zeiss Axiovert 200; Zeiss, Welwyn Garden City, UK). The 100-nm sections were post-stained with lead citrate and uranyl acetate before viewing by transmission electron microscopy (TEM) (Hitachi H-7000 electron microscope; Hitachi, Wokingham, UK).

Alkaline Phosphatase Staining

Staining was performed at 37°C as described previously (6).

Immunocytochemistry

Immunostaining of pro–surfactant protein-C (pSPC) (0.5 μg/ml rabbit polyclonal antibody; Chemicon, Chandlers Ford, UK) was performed on cells that were washed and fixed in 4% paraformaldehyde before antigen retrieval (15 min at 90°C in target retrieval solution; Dako, Ely, UK). Otherwise, cell monolayers were washed and fixed with methanol before treatment with serum-free protein block (Dako) and were probed with antibodies to thyroid transcription factor (TTF)-1 (2 μg/ml, mouse monoclonal; Oncogene, Merck, Nottingham, UK), pan-cytokeratin (10 μg/ml, rabbit polyclonal; Zymed, Invitrogen, Paisley, UK), or an isotype specific control at the same concentration. Immunoreactivity was detected using an indirect streptavidin-biotin method (LSAB kit; Dako) and horseradish peroxidase (HRP). Bound antibody was detected as a brown stain. Photographs were taken using a Sony cyber-shot digital camera (Sony, Basingstoke, UK).

Immunoblotting and Immunofluorescence

Confluent immortal and primary cells were lysed in sample buffer (250 mM Tris, pH 6.8; 10% glycerol; 4% SDS; 2% 2-mercaptoethanol; 0.01% bromophenol blue) and boiled for 10 minutes. Samples were centrifuged before analysis of equal volumes of supernatant. Proteins were resolved using a NuPAGE 10% Bis-Tris gel (Invitrogen, Paisley, UK) with MES running buffer and transferred to a nitrocellulose membrane. The membrane was blocked (5% skimmed milk powder in Tris NaCl; 0.1% Tween-20) for 1 hour at room temperature before being probed with an Ab to caveolin-1 (1:2,000, rabbit polyclonal; BD Transduction Laboratories, BD Biosciences, Oxford, UK), or RAGE (1:500, mouse monoclonal; Chemicon), overnight at 4°C. Proteins were detected by incubation with HRP-conjugated anti-rabbit IgG (Dako) and visualized using enhanced chemiluminescence. For immunofluorescence, confluent immortal cells were fixed in methanol for 20 minutes, washed, then blocked in 2% BSA. Cells were incubated with the same Caveolin-1 Ab as above (10 μg/ml) for 2 hours and then incubated with a secondary Ab conjugated to Texas Red (Santa Cruz Biotech, Inc., Santa Cruz, CA). For nuclear staining, cells were incubated with DAPI (Sigma).

Scanning Ion Conductance Microscopy and Scanning Surface Confocal Microscopy

Scanning surface confocal microscopy (SSCM) combines scanning confocal microscopy with scanning ion conductance microscopy (SICM) (13). SICM is a scanning probe microscopy technique that uses a glass nanopipette as a sensitive probe that detects ion current and uses the current as an interaction signal to control the vertical (z-axis) position of the cell relative to the pipette tip (14). In SSCM the cell is moved up and down in the z direction while it is scanned in the x and y directions, so its surface is always the same distance from the nanopipette (typically, 25–75 nm). A laser beam passed up a high numerical aperture objective is focused just at the tip of the nanopipette, and a pinhole is positioned at the image plane so that the confocal volume is just below the pipette (15). Thus, a fluorescence image of the cell surface is obtained in a single scan, as well as a simultaneously captured image of the cell topography. The cells were examined over a period of 4 hours.

Exposure of Cells to Fluorescent Microspheres

Polystyrene latex microspheres (Sigma) were either positively charged (amine modified) or negatively charged (carboxylate modified). The microspheres were either 50 nm or 1 μm and were labeled with green fluorescent dye. Cells (studied between passages 20 and 60) were grown to confluence (48 h after passage) on coverslips in 24-well tissue culture plates (Costar, Corning Inc.) and then serum starved for 24 hours. The beads were vortexed for 1 minute before diluting in media to generate a 0.006% solution (wt/vol) and sonicated for 1 minute using a sonicating probe (Soniprep 150 MSE; MSE, London, UK), just before addition to the cells, to reduce aggregation. After 18 hours the cell supernatant was removed and the cells washed with PBS to remove any excess beads before fixing with 2% paraformaldehyde. Cells were stained with 1% Evans blue (cell protein, red) and 1 μg/ml DAPI (DNA, blue) and visualized by confocal laser scanning microscopy (Leica TCS-SP; Leica, Milton Keynes, UK).

The number of cells that had internalized beads in five random fields per well was recorded as a percentage of the total number of cells in the field of view. Confocal images were taken of 6 to 12 sections through the cells, depending on cell depth, to establish that the particles were present within the cell cytoplasm and not simply attached to the outside of the cell membrane. It was not possible to determine the number of particles per cell, as the confocal resolution only detects particles that are clustered together, not individual particles.

Time Course of Internalization of Fluorescent Microspheres

Further studies were performed to assess the rate at which 50-nm particles were internalized by primary AT2 and immortal cells. Confluent, serum-starved (24 h) cells were exposed to fluorescently labeled negatively and positively charged polystyrene beads (50 nm) over 24 hours. Beads were vortexed for 1 minute and sonicated for a further minute to produce a uniform suspension, and were diluted to a final concentration of 0.006% wt/vol in medium. The suspension was then added to the cells and particle uptake assessed at 5, 10, 15, and 30 minutes, and at 1, 2, 3, and 24 hours. At each time point the media were removed and the cells washed to remove any particles that had not been internalized. To further reduce the background signal, extracellular fluorescence was quenched using trypan blue. To investigate passive diffusion of particles into cells, parallel studies were performed at 4°C to subdue cell metabolism and inhibit active cellular uptake of particles. Internalized particles were then visualized under a fluorescence microscope, and images were captured from five randomly selected fields of vision. Using SimplePCI software (Digital Pixel, Brighton, UK) it was possible to semi-quantify the levels of particle uptake. Using the captured images, the increase in internalized particles was assessed by measuring the total fluorescence for each field of vision. This was normalized to the unit mass of the original particle exposure. Thus, fluorescence increased in proportion to particle internalization.

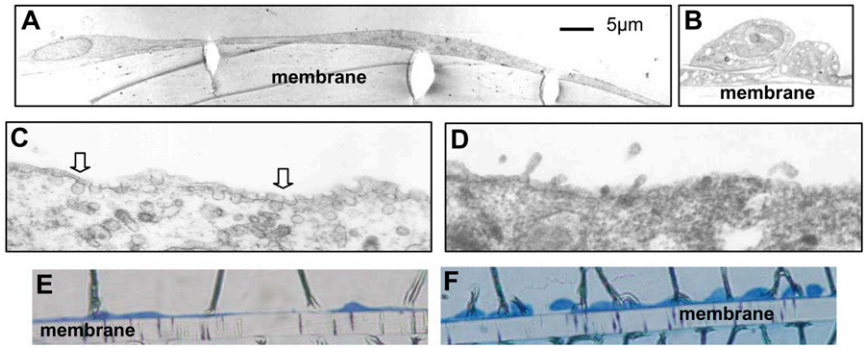

Figure 1. Transmission electron microscopy (TEM) of immortal cells and alveolar type (AT)2 cells grown on Transwell membranes. The immortal cells (*A*) have a thin, flattened appearance, whereas the AT2 cells (*B*) are cuboidal; the *scale bar* relates to *A* and *B*. High-magnification TEM shows vesicles at the surface of the immortal cells (*C*, *arrows*), which are absent from the AT2 cells (*D*). Toluidine blue staining of TEM sections; 10 or 11 AT2 cells (*F*) occupy the same distance (165 μm) as 2 immortalized cells (*E*). Membrane = 10 μm deep.

RESULTS

TEM and SICM

Low-power sections of each cell type show the cuboidal shape of the primary AT2 cells (Figure 1B) and the flattened, thin morphology of the immortal cells (Figure 1A), which resembles that of AT1 cells. Primary AT2 cells contain lamellar bodies and have surface microvilli (Figure 1D), not seen on the immortalized cells. At higher magnification, some immortal cells are shown to contain endosomal vesicles within the cytoplasm and at the cell membrane (Figure 1C). There were no caveolae in the primary AT2 cells (Figure 1D). Toluidine blue staining of TEM sections illustrates how two immortalized cells (Figure 1E) cover the same length of membrane (165 μm) as 10 or more primary AT2 cells (Figure 1F). Thus, each primary AT2 cell covers approximately 15 μm, whereas each immortal cell covers approximately 80 μm in diameter (since TEM cross-sections were rarely less than 80 μm). Live cell imaging using SICM confirmed that the immortal AT1-like cells were flattened, circular cells greater than 40 μm in diameter (Figure 2C), whereas the primary AT2 cells were 15 μm (Figure 2A) and also contained numerous surface microvilli (Figures 2B and 2D), resembling their morphology *in vivo*.

Primary AT2 Cell Markers

TTF-1 is a marker for AT2 cells, whereas AT1 cells are negative (16). Strong nuclear staining for TTF-1 was seen in the primary AT2 cells (Figure 3B), whereas the immortal cells were negative (Figure 3A). Surfactant protein-C maintains reduced surface tension in the alveolus and is unique to AT2 cells (17, 18). Primary AT2 cells were positive (Figure 3D), whereas the immortal cells were negative (Figure 3C) for pSPC. Alkaline phosphatase is a marker of the AT2 cell phenotype in the lung (19). The primary AT2 cells exhibit strong pink positive staining (Figure 3F), whereas the immortal cells were negative (Figure 3E), demonstrating loss of the AT2 cell alkaline phosphatase phenotype, as occurs *in situ*.

Immortal AT1 Cell Markers

Caveolin-1 (Figure 4A) and RAGE (Figure 4C) were detected by immunoblotting of cell lysates from immortal cells but not primary AT2 cells. Immunofluorescent staining of immortal cells for caveolin-1 (Figure 4B) showed this protein as aggregates in the cytoplasm, corresponding with the presence of vesicles in these cells and, together with RAGE, is a marker of AT1 cells (20), suggesting that the immortal cells have an AT1-like cell phenotype. Cytokeratins are the main structural proteins in epithelial cells; the immortal cells displayed pan-cytokeratin staining (Figure 4D), confirming their epithelial phenotype and lack of contamination by capillary endothelial cells.

Particle Internalization

All four types of latex bead were taken up by the immortalized and primary AT2 cells (Figure 5), albeit at very different levels. At the concentrations described in this study there was no toxicity, although we previously observed cell death when high concentrations of amine-modified 50-nm particles were used. Images show a section through the middle of the cells and a composite of all the sections through the cell. The section through the middle of the cell demonstrates that the particles are internalized and not just present on the surface of the cell or between cells. Composite images are particularly important to be able to appreciate the significant uptake of 50-nm negatively

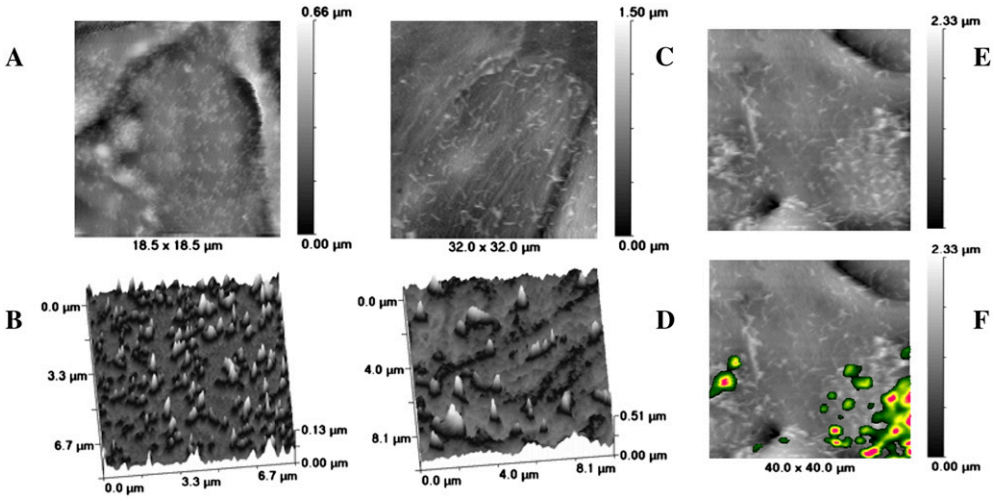

Figure 2. Scanning ion conductance microscopy (SICM) and scanning surface confocal microscopy (SSCM) images of AT2 and immortal cells. (*A*) SICM image of AT2 cell (~ 15 μm diameter) enriched with microvilli, shown at high power in *B*. (*C*) SICM of immortal cells illustrating cellular attenuation, forming flat circular cells that are greater than the 32- and 40-μm *x*-axis of the image, and showing scattered, irregular microvilli, shown at high power in *D*. (*F*) SSCM of immortal cells exposed to fluorescent 50-nm latex particles for 30 minutes; particles are located above areas with microvillar activity, compared with SICM image of the same cell in *E*. The *z*-axis *scale bar* is located on the *right* of *A*, *C*, *E*, and *F*.

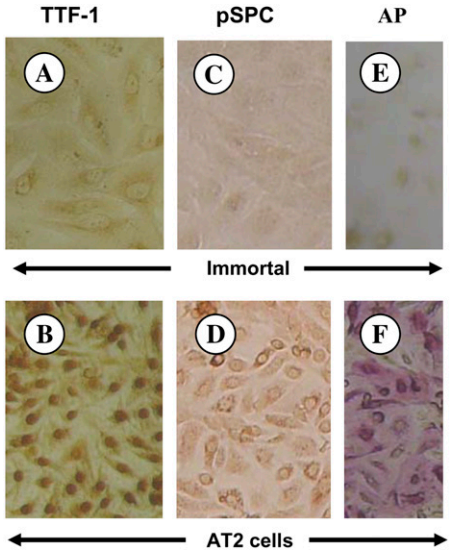

Figure 3. Thyroid transcription factor (TTF)-1 and pro–surfactant protein-C (pSPC) immunostaining of immortal (*A, C*) and AT2 epithelial cells (*B, D*). Cells were incubated with an antibody to TTF-1 (*A, B*) or pSPC (*C, D*). AT2 cells were positive for TTF-1 (*B*, nuclear stain) and for pSPC (*D*), whereas immortal cells were negative for both TTF-1 (*A*) and pSPC (*C*). AT2 cells showed strong pink positive alkaline phosphatase staining (*F*), whereas the immortal cells were negative (*E*).

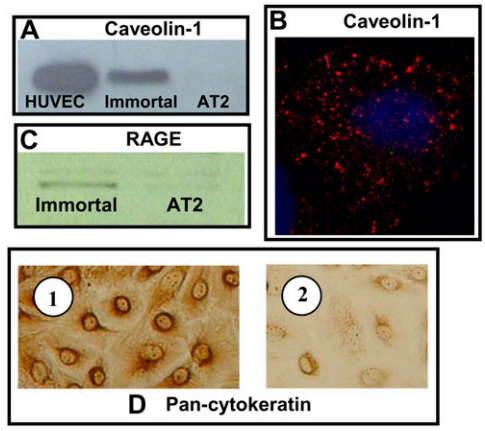

Figure 4. Immunoblotting for caveolin-1 and RAGE and immunostaining for caveolin-1 and pan-cytokeratin. (*A*) Caveolin-1. Immortal cell lysates were positive, while AT2 cells were negative, for caveolin-1. HUVEC lysate was used as a positive control. (*B*) Confocal microscopy of immortal cells immunostained for caveolin-1. Caveolin-1 visualized as *red aggregates* in the cytoplasm; nucleus is *blue*. (*C*) RAGE. Immortal cell lysates were positive, while AT2 cells were negative, for RAGE. (*D*) Pan-cytokeratin immunoreactivity. Immortal cell monolayers were positive for pan-cytokeratin antibody (1), confirming an epithelial phenotype. Isotype control (*2*).

charged particles by the immortal cells (Figure 5). In these confocal studies the numbers of cells containing particles was quantified, as this method cannot accurately estimate the total mass or numbers of nanoparticles due to the low resolution. Thus, less than 8% of the primary AT2 cells internalized the particles (Figure 6). In contrast, at least 44% of the immortal cells internalized the particles ($P < 0.001$). Significantly more of the immortal cells internalized negatively charged particles (75%) compared with the positively charged particles (< 55%; $P < 0.05$). One-micrometer particles were found to be perinuclear in the immortal cells, in contrast to primary AT2 cells, where these particles were distributed throughout, regardless of charge. Regarding location of the nanoparticles, negatively charged particles were usually in the perinuclear region, whereas positively charged particles were less dense and not obviously in the perinuclear zone. SSCM of live cells showed that internalization of 50-nm particles by immortalized cells occurred over central regions of the cells (Figure 2F) that had become enriched with microvilli on exposure to the particles (Figure 2E). This process could be observed in real time and was rapid, with about 40% disappearing within 30 minutes. Thus further studies were performed, over time, on the immortal cells using semiquantitive, light microscopy, which took account of the total signal rather than individual cell uptake.

Quantification of negative, 50-nm particle uptake by immortalized cells using light microscopy showed a rapid increase in cellular fluorescence over the first 15 minutes (Figure 6C). The rate at which particles were internalized slowed over the subsequent 3.75 hours but still increased significantly ($P < 0.0021$). Similarly, there was a significant increase in uptake of positively charged 50-nm beads over the same time course ($P < 0.0013$). Over the following 21 hours the number of internalized particles continued to increase, at a reduced rate, reaching approximately 2.5-fold and 1.64-fold that at 4 hours for negatively and positively charged particles, respectively ($P < 0.001$; data not shown). The rate of uptake of negatively charged particles was significantly higher than that for positively charged particles (Figure 6C; 5 and 10 min, $P < 0.0002$; 15, 30, and 60 min, $P < 0.0001$; 120 and 180 min, $P < 0.002$; 240 min, $P < 0.0006$), being approximately 4.4- and 1.8-fold that of the positively charged particles at 30 minutes and at 4 hours, respectively. When the study was performed at 4°C, by 4 hours, intracellular fluorescence reached 71% and 57%, respectively, of the negative and positive particle uptake observed at 37°C, suggesting a significant degree of passive uptake. It was not possible to measure particle uptake by primary AT2 cells, which was very low, and the fluorescence was undetectable using light microscopy.

DISCUSSION

We have immortalized primary human AT2 cells by retroviral transduction with hTERT and U19tsA58. Unlike primary AT2 cells, immortal cells were negative for alkaline phosphatase, suggesting that immortalization had driven the AT2 cells toward an AT1 cell phenotype. Further characterization by TEM showed that the AT2 cells were typically cuboidal, containing lamellar bodies, with apical microvilli, as described by us previously, resembling AT2 cells *in vivo* (6, 21–23). In contrast, the immortal cells did not contain lamellar bodies and displayed a flattened morphology. Very low power examination of toluidine blue–stained cells showed that each immortalized cell extended for up to 80 μm in diameter, while the the cuboidal AT2 cells were only about 15 μm. Thus, the immortalized cells resembled AT1 cells *in vivo*, where they spread thinly (0.2–0.3 μm deep) over the alveolus in close contact with the underlying endothelium to allow gas exchange, while covering a large area (24). Complimentary SCIM imaging of live human primary AT2 cells confirmed the cuboidal morphology and surface microvilli observed using SEM of AT2 cells *in situ* (22, 23). In contrast, SICM of live immortal cells revealed a flattened, circular morphology of greater than 40 μm diameter, resembling SEM of AT1 cells *in situ* (22, 23). We suggest that immortalization of primary human AT2 cells has driven the cells toward an AT1-like cell phenotype.

Pulmonary AT1 cells contain numerous small vesicles in the plasma membrane, including caveolae and clathrin-coated pits,

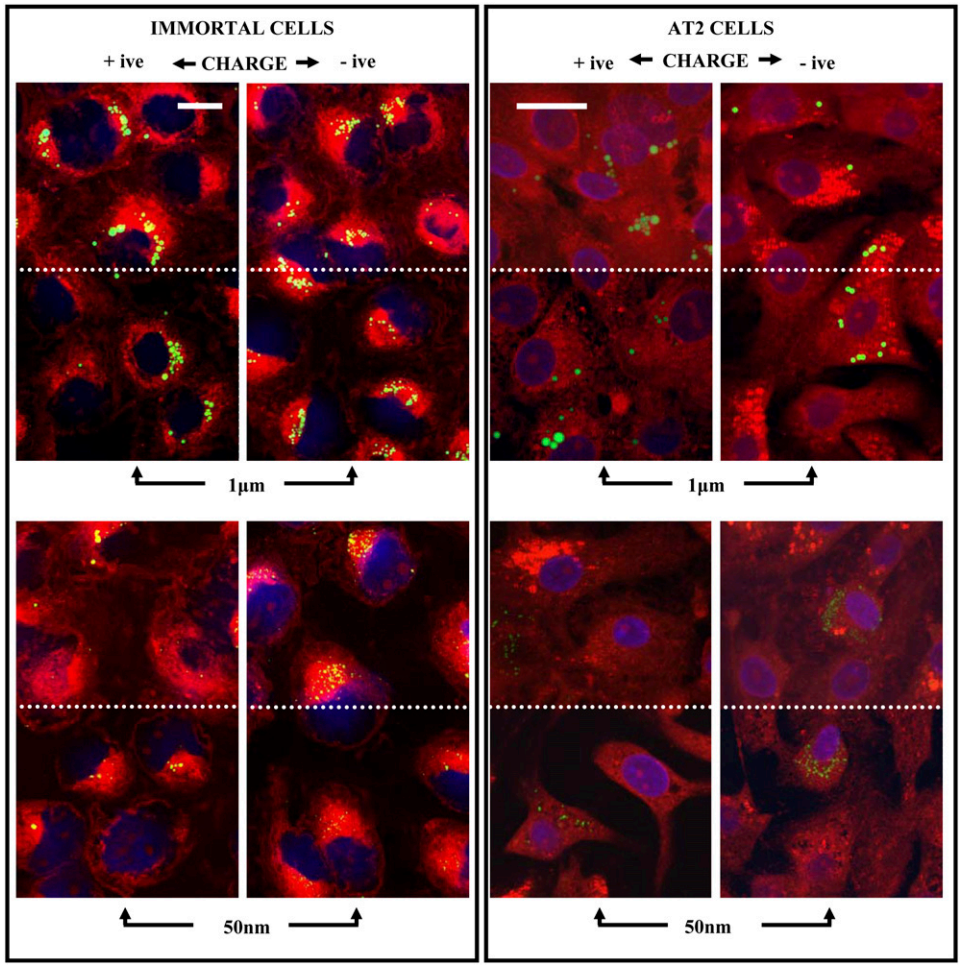

Figure 5. Immortal and AT2 cells were exposed to positively and negatively charged 1-μm and 50-nm fluorescent latex beads for 18 hours, fixed, stained, and viewed by confocal microscopy. The *top half* of each image (above the *dotted line)* is a composite of all the sections to (*1*) illustrate the presence of high numbers of 50-nm particles, particularly in the immortal cells exposed to negatively charged particles; and (*2*) show absence of particles between cells. The *bottom half* of each image (below the *dotted line*) shows a focal plane through the middle of the cells, demonstrating internalization of beads. The figures for AT2 cells are shown at a higher magnification to focus in on the relatively low number of cells containing particles as well as to highlight the presence of the nanoparticles. This difference in magnification is denoted by the length of the *white bar* in the *top left panel* for each cell type, which denotes 20 μm.

which pinch off from the plasma membrane to form vesicles, transporting their contents into/through the cytoplasm. Biochemically, caveolae are defined by their major structural protein, caveolin-1 (25, 26). In this study, the presence of vesicles in some cells and positive immunoblotting for caveolin-1 in immortalized cells supports the presence of caveoli, a characteristic of AT1, but not AT2, cells (27–29). Positive pancytokeratin excluded contamination by endothelial cells, which also contain vesicles and caveoli. Furthermore, immortalized cells, but not primary AT2 cells, were positive for RAGE, which has been described to be unique to AT1 lung cells (20). Little is known about the function of RAGE; however, overexpression of RAGE in HEK293 cells shows that RAGE promotes the adherence and spreading of epithelial cells onto collagen (30), suggesting a similar role in AT1 cells. Nuclear TTF-1 was not expressed by immortalized cells; it regulates transcription of surfactant proteins A, B, and C (31–34), and AT2, but not AT1, cells express TTF-1 *in situ* (16). TTF-1 is also required for lung morphogenesis; overexpression results in AT2 cell hyperplasia and is suggested to inhibit differentiation of AT2 cells to the AT1 phenotype and alveolarization (35). Although it is possible to isolate primary rodent AT1 cells, to our knowledge, there are no methods to isolate human AT1 cells (24). An alternative is to use primary AT2 cells that have lost their phenotype *in vitro* to resemble AT1 cells (28, 36). Recently, AT1-like cells have been obtained from transdifferentiating human fetal primary AT2 cells (37). However, the authors did not present evidence that these cells could be passaged as can the immortal cells herein. We suggest that the immortalized, AT1-like cells described in the present study offer another alternative model to investigate the role of human AT1 cells in pulmonary homeostasis. In the present study, we have used the cells up to passage 60 with no loss of behavioral phenotype. These cells, along with other models, could prove to be a useful, *in vitro* tool to further investigate the role of human AT1 cells, of which currently relatively little is known.

The pulmonary epithelium is one of the first sites of delivery of inhaled organic and inorganic particles. Evidence suggests that increased cardiovascular morbidity and mortality during episodes of air pollution is due to the fine and ultrafine particulate components, which readily access the respiratory units, where they may set up local inflammation and responses that favor blood clotting. Alternatively, several *in vivo* studies suggest that there is translocation of nano-sized particles into the vasculature, where they may react within the circulation, or reach other compartments of the body (38, 39). We hypothesized that the epithelial cells would be involved and used the immortal, AT1-like cells and primary AT2 cells to investigate this idea *in vitro*.

A striking discovery was that immortal, AT1-like cells avidly internalized all types of polystyrene particles, although, using confocal microscopy, significantly more cells were found to internalize negatively charged particles; additional semiquantitative light microscopy studies of 50-nm particles confirmed preferential internalization of particles, particularly negatively charged, by the immortal, AT1-like cells. In contrast only a small percentage of primary AT2 cells internalized particles. SSCM of live cells at high magnification also showed that only immortal, AT1-like cells internalized 50-nm particles, which initially deposited at the cell margins and then relocated to central regions

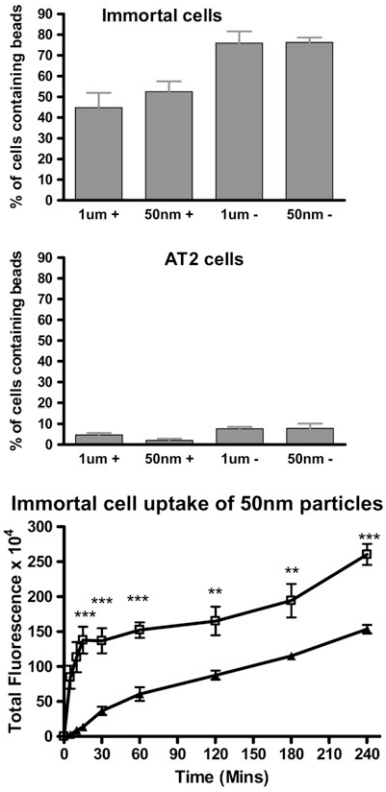

Figure 6. Immortal cells and AT2 cells were exposed to positively and negatively charged, 1-μm and 50-nm fluorescent latex particles. Cells were examined by confocal microscopy and the number of cells which had internalized beads was recorded. Data are shown as *bar graphs*, expressed as percentage of total cells containing beads, mean ± SE. Uptake of 50-nm fluorescent particles by immortal cells over time (240 min) was determined by light microscopy and image analysis as total fluorescence; *open squares*, negatively charged particles; *solid triangles*, positively charged particles (**$P < 0.002$, ***$P < 0.0002$).

that became enriched with microvilli before particle internalization, suggesting an active process involving microvilli. This is interesting, since fetal AT2-derived AT1 cells also exhibited microvilli (37). Our study suggests that AT1 cells may exhibit microvilli when activated. There was no evidence in this preliminary study that monolayer integrity was compromised, or that particles passed between cells; monolayer behavior is the subject of ongoing investigations. These *in vitro* studies suggest that the AT1 cells could be crucial in translocation of inhaled fine and nano-sized particles across the lung and that the AT2 cells only have a relatively small role to play in this process.

We were surprised by the marked difference in particle uptake by these two cell types. Furthermore, cells either took up particles or did not, depending on surface charge or cell type, suggesting that cell-specific processes are involved. There are many putative mechanisms of cellular uptake and/or translocation of nanoparticles across the alveolar gas–blood barrier. Numerous studies *in vivo* and *in vitro* highlight the multifactorial issues that influence particle–cell interactions (40). These include the physicochemical properties of the particles, the type of target cell, and the acellular milieu in which the particles are bathed (e.g., lung secretions, blood). For example, after inhalation, 22-nm titanium dioxide particles were discovered within epithelial and endothelial cells, in fibroblasts as well as between collagen fibrils and in the connective tissue, and it was suggested that transfer was by passive diffusion; this was supported using an *in vitro* model (38). The current study also indicates that passive uptake is one important mechanism in AT1 cells, particularly for negatively charged particles. In contrast, others have shown that inhaled gold nanoparticles (5–8nm) were mostly located in vesicles in the cytoplasm of macrophages and AT1 cells, pointing to endosomal uptake (41). In addition to interaction with, and uptake by, target cells, translocation of particles across the alveolar gas–blood barrier depends on size, surface charge, and opsonization (recently reviewed in Refs. 40 and 42), and is as yet unpredictable. This study also indicates that surface charge, cell phenotype, and specific cell mechanisms are important, as passive mechanisms only accounted for 50 to 70% of the total particle uptake by AT1-like cells. Furthermore, the very low levels of particle uptake by AT2 cells indicate significant cellular differences that facilitate passive uptake by AT1, but not AT2, cells.

Other pathways might involve vesicular transport. Albumin uptake by rat lung AT1 and AT2 cells has been ascribed to clathrin-mediated endocytosis and is higher in AT2 cells (43). Caveolin-mediated mechanisms were also studied, but they were found to be irrelevant (43). In the current study, although we could visualize caveolin-1–stained bodies in immortal, AT1-like cells using confocal microscopy, these bodies never co-localized with the latex particles (data not shown), suggesting that different mechanisms exist (e.g., clathrin-mediated endocytosis or non–caveolin-, non–clathrin-mediated uptake). Alternatively, if particles were internalized via caveoli, it is possible that the particles were transferred into the cytosol or into another organelles, such as the endoplasmic reticulum. The mechanisms of uptake of inhaled, organic, and inorganic nanoparticulate material will not necessarily equate with the mechanisms involved in protein (e.g., albumin) transport and are likely to be complex. We are currently investigating these possibilities further.

We were surprised that the 50-nm and 1-μm particles were internalized by equal numbers of immortal, AT1-like cells. These were monocultures and thus the cells were not "protected" by alveolar macrophage phagocytosis and clearance of the particles. In this respect, inhaled, larger particles can be recovered from the lung by bronchoalveolar lavage more readily than nano-sized particles (44). The micrometer-sized particles are mostly associated with macrophages leading to the view that macrophages readily internalize and remove particles in the micrometer size range, they may not always recognize and clear nanoparticles unless they form larger structures by aggregation or agglomeration. Nanoparticles may bypass macrophages, impact on, and interact with, the epithelial cells, enhancing the likelihood of epithelial cell uptake (45). Inhaled nanoparticles cannot be completely recovered by bronchoalveolar lavage, being present in the lung tissue; this supports the concept that they are translocated through epithelial cells and/or relocated to other compartments. In this study of epithelial monolayers, in the absence of macrophages, internalization of 1-μm latex particles by epithelial cells may reflect *in vitro* opportunity rather than a normal function that exists *in vivo*. However, recent studies using triple co-cultures of epithelial cells (A549), dendritic cells, and macrophages to replicate the airway barrier to study the passage of 1-μm particles discovered particles within all cell types and furthermore appeared to be actively transferred between different dendritic cells and macrophages (46, 47). It would be interesting to discover how particle uptake by the cells described in the present study may be influenced by the presence of such immune effector cells. These are the subject of other ongoing investigations.

References

1. Uhal BD. Cell cycle kinetics in the alveolar epithelium. *Am J Physiol* 1997;272:L1031–L1045.
2. Crapo JD, Barry BE, Gehr P, Bachofen M, Weibel ER. Cell number and cell characteristics of the normal human lung. *Am Rev Respir Dis* 1982;125:740–745.
3. Kim KJ, Malik AB. Protein transport across the lung epithelial barrier. *Am J Physiol Lung Cell Mol Physiol* 2003;284:L247–L259.
4. Borok Z, Liebler JM, Lubman RL, Foster MJ, Zhou B, Li X, Zabski SM, Kim KJ, Crandall ED. Na transport proteins are expressed by rat alveolar epithelial type I cells. *Am J Physiol Lung Cell Mol Physiol* 2002;282:L599–L608.

5. Johnson MD, Widdicombe JH, Allen L, Barbry P, Dobbs LG. Alveolar epithelial type I cells contain transport proteins and transport sodium, supporting an active role for type I cells in regulation of lung liquid homeostasis. *Proc Natl Acad Sci USA* 2002;99:1966–1971.
6. Witherden IR, Vanden Bon EJ, Goldstraw P, Ratcliffe C, Pastorino U, Tetley TD. Primary human alveolar type II epithelial cell chemokine release: effects of cigarette smoke and neutrophil elastase. *Am J Respir Cell Mol Biol* 2004;30:500–509.
7. O'Hare MJ, Bond J, Clarke C, Takeuchi Y, Atherton AJ, Berry C, Moody J, Silver AR, Davies DC, Alsop AE, *et al.* Conditional immortalization of freshly isolated human mammary fibroblasts and endothelial cells. *Proc Natl Acad Sci USA* 2001;98:646–651.
8. Churg A, Brauer M, Vedal S, Stevens B. Ambient mineral particles in the small airways of the normal human lung. *J Environ Med* 1999;1: 39–45.
9. Dockery DW. Epidemiologic evidence of cardiovascular effects of particulate air pollution. *Environ Health Perspect* 2001;109:483–486.
10. Dockery DW, Pope CA III, Xu X, Spengler JD, Ware JH, Fay ME, Ferris BG Jr, Speizer FE. An association between air pollution and mortality in six US cities. *N Engl J Med* 1993;329:1753–1759.
11. Boland S, Baeza-Squiban A, Fournier T, Houcine O, Gendron MC, Chevrier M, Jouvenot G, Coste A, Aubier M, Marano F. Diesel exhaust particles are taken up by human airway epithelial cells in vitro and alter cytokine production. *Am J Physiol* 1999;276:L604–L613.
12. Muhlfeld C, Rothen-Rutishauser B, Blank F, Vanhecke D, Ochs M, Gehr P. Re-evaluation of pulmonary titanium dioxide nanoparticle distribution using the "relative deposition index": evidence for clearance through microvasculature. *Part Fibre Toxicol* 2007;4:7.
13. Korchev YE, Bashford CL, Milovanovic M, Vodyanoy I, Lab MJ. Scanning ion conductance microscopy of living cells. *Biophys J* 1997; 73:653–658.
14. Gorelik J, Shevchuk A, Ramalho M, Elliott M, Lei C, Higgins CF, Lab MJ, Klenerman D, Krauzewicz N, Korchev Y. Scanning surface confocal microscopy for simultaneous topographical and fluorescence imaging: application to single virus-like particle entry into a cell. *Proc Natl Acad Sci USA* 2002;99:16018–16023.
15. Shevchuk AI, Gorelik J, Harding SE, Lab MJ, Klenerman D, Korchev YE. Simultaneous measurement of Ca2+ and cellular dynamics: combined scanning ion conductance and optical microscopy to study contracting cardiac myocytes. *Biophys J* 2001;81:1759–1764.
16. Morotti RA, Gutierrez MC, Askin F, Profitt SA, Wert SE, Whitsett JA, Greco MA. Expression of thyroid transcription factor-1 in congenital cystic adenomatoid malformation of the lung. *Pediatr Dev Pathol* 2000;3:455–461.
17. Kalina M, Mason RJ, Shannon JM. Surfactant protein C is expressed in alveolar type II cells but not in Clara cells of rat lung. *Am J Respir Cell Mol Biol* 1992;6:594–600.
18. Beers MF, Kim CY, Dodia C, Fisher AB. Localization, synthesis, and processing of surfactant protein SP-C in rat lung analyzed by epitope-specific antipeptide antibodies. *J Biol Chem* 1994;269:20318–20328.
19. Edelson JD, Shannon JM, Mason RJ. Alkaline phosphatase: a marker of alveolar type II cell differentiation. *Am Rev Respir Dis* 1988;138: 1268–1275.
20. Shirasawa M, Fujiwara N, Hirabayashi S, Ohno H, Iida J, Makita K, Hata Y. Receptor for advanced glycation end-products is a marker of type I lung alveolar cells. *Genes Cells* 2004;9:165–174.
21. Witherden IR, Tetley TD. Isolation and culture of human type II pneumocytes. In: Rogers DF, Donelly LE, editors. Human airway inflammation: sampling techniques and analytical protocols. Totowa: Humana Press; 2001. pp. 137–146.
22. Nagai A, Thurlbeck WM. Scanning electron microscopic observations of emphysema in humans. a descriptive study. *Am Rev Respir Dis* 1991; 144:901–908.
23. Wang NS, Thurlbeck WM. Scanning electron microscopy of the lung. *Hum Pathol* 1970;1:227–231.
24. Williams MC. Alveolar type I cells: molecular phenotype and development. *Annu Rev Physiol* 2003;65:669–695.
25. Couet J, Belanger MM, Roussel E, Drolet MC. Cell biology of caveolae and caveolin. *Adv Drug Deliv Rev* 2001;49:223–235.
26. Schnitzer JE, Oh P, Pinney E, Allard J. Filipin-sensitive caveolae-mediated transport in endothelium: reduced transcytosis, scavenger endocytosis, and capillary permeability of select macromolecules. *J Cell Biol* 1994;127:1217–1232.
27. Campbell L, Hollins AJ, Al Eid A, Newman GR, von Ruhland C, Gumbleton M. Caveolin-1 expression and caveolae biogenesis during cell transdifferentiation in lung alveolar epithelial primary cultures. *Biochem Biophys Res Commun* 1999;262:744–751.
28. Fuchs S, Hollins AJ, Laue M, Schaefer UF, Roemer K, Gumbleton M, Lehr CM. Differentiation of human alveolar epithelial cells in primary culture: morphological characterization and synthesis of caveolin-1 and surfactant protein-C. *Cell Tissue Res* 2003;311:31–45.
29. Newman GR, Campbell L, von Ruhland C, Jasani B, Gumbleton M. Caveolin and its cellular and subcellular immunolocalisation in lung alveolar epithelium: implications for alveolar epithelial type I cell function. *Cell Tissue Res* 1999;295:111–120.
30. Demling N, Ehrhardt C, Kasper M, Laue M, Knels L, Rieber EP. Promotion of cell adherence and spreading: a novel function of RAGE, the highly selective differentiation marker of human alveolar epithelial type I cells. *Cell Tissue Res* 2006;323:475–488.
31. Bohinski RJ, Di Lauro R, Whitsett JA. The lung-specific surfactant protein B gene promoter is a target for thyroid transcription factor 1 and hepatocyte nuclear factor 3, indicating common factors for organ-specific gene expression along the foregut axis. *Mol Cell Biol* 1994;14: 5671–5681.
32. Bruno MD, Bohinski RJ, Huelsman KM, Whitsett JA, Korfhagen TR. Lung cell-specific expression of the murine surfactant protein A (SP-A) gene is mediated by interactions between the SP-A promoter and thyroid transcription factor-1. *J Biol Chem* 1995;270:6531–6536.
33. Kelly SE, Bachurski CJ, Burhans MS, Glasser SW. Transcription of the lung-specific surfactant protein C gene is mediated by thyroid transcription factor 1. *J Biol Chem* 1996;271:6881–6888.
34. Yan C, Sever Z, Whitsett JA. Upstream enhancer activity in the human surfactant protein B gene is mediated by thyroid transcription factor 1. *J Biol Chem* 1995;270:24852–24857.
35. Wert SE, Dey CR, Blair PA, Kimura S, Whitsett JA. Increased expression of thyroid transcription factor-1 (TTF-1) in respiratory epithelial cells inhibits alveolarization and causes pulmonary inflammation. *Dev Biol* 2002;242:75–87.
36. Campbell L, Abulrob AN, Kandalaft LE, Plummer S, Hollins AJ, Gibbs A, Gumbleton M. Constitutive expression of p-glycoprotein in normal lung alveolar epithelium and functionality in primary alveolar epithelial cultures. *J Pharmacol Exp Ther* 2003;304:441–452.
37. Foster CD, Varghese LS, Skalina RB, Gonzales LW, Guttentag SH. In vitro transdifferentiation of human fetal type II cells toward a type I–like cell. *Pediatr Res* 2007;61:404–409.
38. Geiser M, Rothen-Rutishauser B, Kapp N, Schurch S, Kreyling W, Schulz H, Semmler M, Im Hof V, Heyder J, Gehr P. Ultrafine particles cross cellular membranes by nonphagocytic mechanisms in lungs and in cultured cells. *Environ Health Perspect* 2005;113:1555–1560.
39. Nemmar A, Vanbilloen H, Hoylaerts MF, Hoet PH, Verbruggen A, Nemery B. Passage of intratracheally instilled ultrafine particles from the lung into the systemic circulation in hamster. *Am J Respir Crit Care Med* 2001;164:1665–1668.
40. Unfried K, Albrecht C, Klotz LO, Von Mikecz A, Grether-Beck S, Schins RPF. Cellular responses to nanoparticles: target structures and mechanisms. *Nanotoxicology* 2007;1:52–71.
41. Takenaka S, Karg E, Kreyling WG, Lentner B, Moller W, Behnke-Semmler M, Jennen L, Walch A, Michalke B, Schramel P, *et al.* Distribution pattern of inhaled ultrafine gold particles in the rat lung. *Inhal Toxicol* 2006;18:733–740.
42. Oberdorster G, Stone V, Donaldson K. Toxicology of nanoparticles: a historical perspective. *Nanotoxicology* 2007;1:2–25.
43. Ikehata M, Yumoto R, Nakamura K, Nagai J, Takano M. Comparison of albumin uptake in rat alveolar type II and type I-like epithelial cells in primary culture. *Pharm Res* 2008;25:913–922.
44. Ferin J, Oberdorster G, Penney DP. Pulmonary retention of ultrafine and fine particles in rats. *Am J Respir Cell Mol Biol* 1992;6:535–542.
45. Oberdorster G, Oberdorster E, Oberdorster J. Nanotoxicology: an emerging discipline evolving from studies of ultrafine particles. *Environ Health Perspect* 2005;113:823–839.
46. Rothen-Rutishauser BM, Kiama SG, Gehr PA. Three-dimensional cellular model of the human respiratory tract to study the interaction with particles. *Am J Respir Cell Mol Biol* 2005;32:281–289.
47. Blank F, Rothen-Rutishauser B, Gehr P. Dendritic cells and macrophages form a transepithelial network against foreign particulate antigens. *Am J Respir Cell Mol Biol* 2007;36:669–677.